Temperature Dependence of the Charge Transport in a C_{60} based Organic Field Effect Transistor

Mujeeb Ullah [1], Th .B. Singh [2], G. J. Matt [2], C. Simbruner[1], G. Hernandz-Sosa[1], S. N. Sariciftci [2], H. Sitter [1]

[1] Institute of Semiconductor and Solid State Physics, JKU Linz, Austria.
[2] Linz Institute of Organic Solar Cells, JKU Linz, Austria.

Abstract. We studied the temperature dependence of the electron transport in C_{60} based Organic Field Effect Transistors (OFETs). On the spin-coated bottom gate dielectric, the semi-conducting C_{60} thin-film has been grown by standard evaporation technique. Device parameters as the threshold voltage, the field effect mobility and the activation energy of the electron transport were determined in the temperature range from 300 K to 77 K. The field effect mobility obeys the Meyer-Neldel Rule (MNR), which is an empirical relation between activation energy and the mobility prefactor.

1. Introduction

The charge transport mechanism in organic field effect transistors (OFET) has been subject of research for some years now [1-11]. Although the temperature (T) and gate voltage (V_G) dependence of the charge carrier mobility (μ_{FE}) of OFETs has been reported [1-12], the observed thermally activated behaviour of charge transport mechanisms in these organic devices is still not fully understood. It is even difficult to obtain an accurate picture of the nature of the transport due to large variations in the experimental data on even nominally the same samples [1-11].

Many organic materials have been reported to follow the Meyer-Neldel Rule (MNR) which is a phenomenological model to describe the observed temperature dependence of the mobility.

The thermally activated behavior of the field effect mobility can be described as [3, 4, 7, 8, 10, 13- 15]

$$\mu = \mu_o \exp\left(\frac{-E_A}{k_B T}\right) \qquad (1)$$

where E_A is the variable activation energy, T is the absolute temperature, k_B is Boltzmann constant and μ_o is a prefactor, which can be found empirically. This prefactor also depends on E_A. Equation (2) which gives the relation between the mobility prefactor (μ_o) and E_A is called the MNR.

$$\mu_o = \mu_{oo} \exp\left(\frac{E_A}{k_B T_{MN}}\right) \qquad (2)$$

Inserting equation (2) into (1) gives:

$$\mu = \mu_{oo} \exp\left[-E_A\left(\frac{1}{k_B T} - \frac{1}{k_B T_{MN}}\right)\right] \qquad (3)$$

Which means, that at $T=T_{MN}$ the mobility becomes independent of E_A and is called μ_{MN}. E_A also depends on the applied V_G. Consequently, if μ is plotted versus $1/T$ for different V_G a common crossing point must be obtained at (μ_{MN}, $1/T_{MN}$).

The MNR has been observed in a wide variety of physical, chemical and biological processes [4, 7, 8]. However, the microscopic origin of the MNR and therefore, the physical meaning of E_{MN}, are still a topic of discussion [4, 7-9].

Among the n-type organic semiconductors, fullerenes with a symmetric structure and low ionization potential show a relatively high charge carrier mobility 0.6-6 $cm^2/V^{-1}s^{-1}$. [1, 5] Therefore we selected C_{60} based OFETs for our investigations.

2. Experimental Methods

The device scheme of the OFET employed is shown in the inset of Fig.1 (a). Details of device fabrication of the C_{60} OFETs are reported previously [1, 5]. The deposition of the C_{60} was done at RT using a Leybold Univex system at base pressure of 10^{-6} mbar. The completed devices were loaded in the Oxford cryostat under N atmosphere inside the glove box to avoid exposure to ambient conditions.

The measurements were conducted in small temperature steps of 10K in the range from 300K to 77K. Every temperature step was kept 60 minutes so that the device got thermally stabilized. The output and transfer measurements were recorded by smu Agilent 2000.

3. Results and Discussion

Fig. 1. Shows the output characteristics of the device at 300K and 77K at gate voltages of 20V, 40V, and 60V.

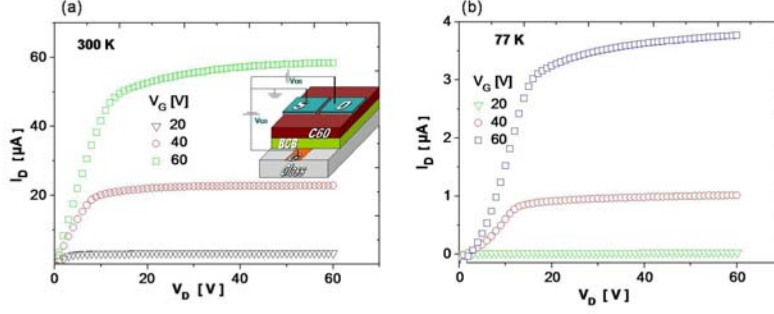

Fig. 1. The output characteristics of the OFET device shown at different gate voltages (a) at 300 K. (b) at 77 K

The transfer characteristics in the linear regime as well as in the saturation regime are shown in Fig. 2 (a) and (b) respectively.

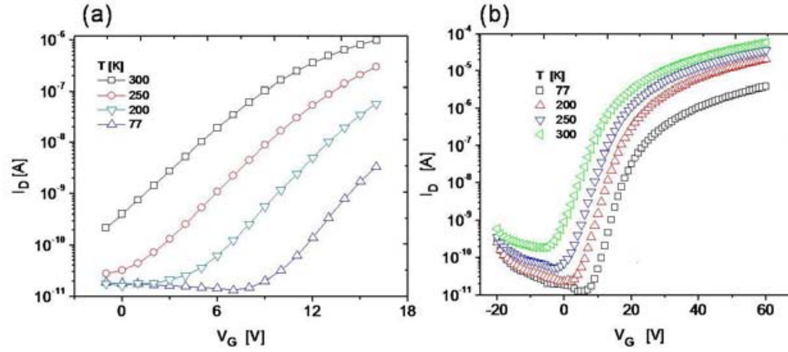

Fig. 2. Transfer characteristics of the C_{60} FET at different temperatures. (a) In the linear regime for V_D=2V and (b) in the saturation regime for V_D=60V.

Without taking into account the contact resistance the drain current (I_D) can be described in the linear regime as function of V_G by the following equation.

$$I_D\Big|_{V_D=constt.} = \frac{W}{L}\ \mu_{FE}\ C_i\, V_D\,(V_G - V_{th.}) \qquad (4)$$

where W and L are the width and length of transistor channel, C_i the capacitance of the dielectric layer and V_{th} the threshold voltage. In the linear regime, the applied gate field is much larger than the in-plane drift field, which results in an approximately uniform density of charge carriers in the active channel. Using equation (4), μ_{FE} can be evaluated from the local slopes of the transfer characterization (see Fig. 2(a). The obtained μ_{FE} in the linear regime is plotted as a function of V_G in Fig. 3 for different temperatures

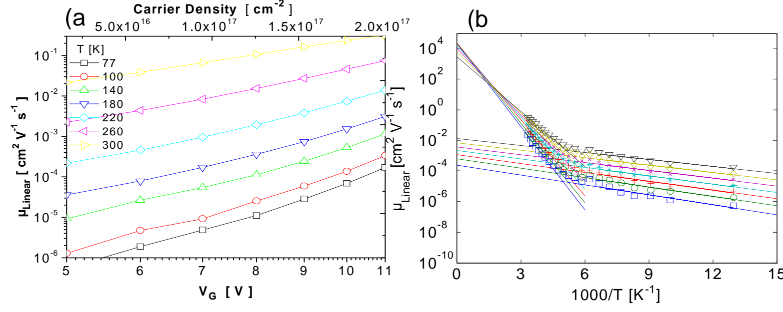

Fig. 3. (a) μ_{FE} in the linear regime as a function of carrier density and the V_G at different T.(b) Arrhenius plot of field effect mobility in linear regime at gate voltages of 5-11V.

This set of data can be converted into an Arrhenius plot as shown in Fig. 3(b) for gate voltages between5 and 11V. The mobility data can now be analyzed by using the MNR described in equation (3). From the slopes of the fit to data points activation energies for the mobility can be calculated for each gate voltage. The results are summarized in Fig. 4(a). The Arrhenius plot of Fig 3(b) can be fitted by two different lines for each V_G depending on the temperature range taken into account. Therefore we obtained two E_A for each V_G depending on the temperature range. The explanation of different E_A in the different ranges of T is unclear, although it has also been observed previously in sexithiophene (6T) and octothiophene (8T) [2].

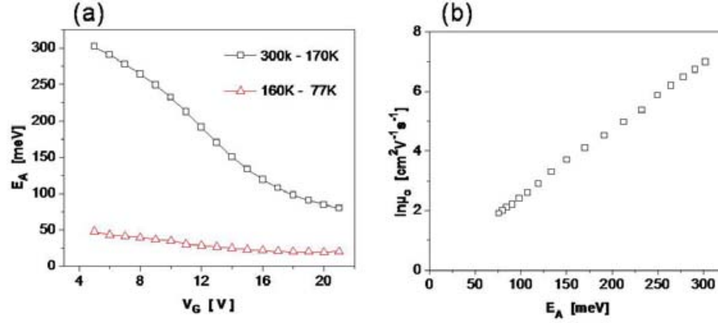

Fig. 4. (a) V_G dependent E_A evaluated using the data from Fig.4 (a) in two different ranges of T. (b) Plot of μ_o verses E_A using the data from Fig.3 (b).

Following the MNR we can deduce from the common intersect of all the fits in Fig. 3(b) the μ_{MN} =2.45cm^{2}V^{-1}s^{-1} and the T_{MN}=480K which corresponds to an E_{MN}=1/ (kB T_{MN}) = 41meV.

Finally the extrapolation of the fitting lines in Fig. 3(b) for infinite temperature gives the prefactor μ_o as defined in the equation (1) for each E_A. The data are summarized in Fig. 4(b).

Such an observation of strong V_G and T dependent E_A can be explained using the multi trap and release model which assumes a semiconductor with Fermi level closer to the band edge and upon applying V_G the Fermi level moves through the distribution of band tail states. As a result E_A is reduced as the density of injected charge carriers are increased above the mobility edge [4, 6-11].

4. Conclusions

Organic field effect transistors were fabricated based on C60 layers. The temperature dependence of μ_{FE} was investigated for different V_G. μ_{FE} is found to be thermally activated with activation energies strongly dependent on the applied V_G. Upon extrapolation of the data in the Arrhenius plot to infinite temperature in the Meyer-Neldel formalism, T_{MN}=480K and μ_{MN}=2.45cm^{2}V^{-1}s^{-1} can be extracted. The observed temperature dependence of μ_{FE} can be explained by empirical MNR, which is based on the assumption of an exponential density of states distribution.

Acknowledgements. The work was supported by Austrian Science Foundation (FWF) within the National Research Network (NFN) "Interface controlled and Functionalized Organic Films".

References

1. Th. B. Singh, N. S. Sariciftci, H. Yang, L. yang, B. Plochberger and H. Sitter, *Appl. Phys. Lett*. 90, 231512 (2007)
2. G. Horowitz, R. Hajlaoui, R. Bourguiga, M. Hajlaoui, *Synth. Met*. 101, 401-404 (1999).
3. J. Paloheimo and H. Isotalo, *Synth. Met*. **55**, 3185 (1993).
4. P. Stallinga and H. L. Gomes, *Organic Electronics*. 7, 529-599 (2006).
5. Th. B. Singh, N. Marjanovic, G. J. Matt, S. Günes, N. S. Sariciftci, A. Montaigne Ramil, A. Andreev, H. Sitter, R. Schwödiauer and S. Bauer, *Organic Elec*. 6, 105-110 (2005)
6. G. Horowitz, R. Hajlaoui and P. Delannoy J. Phys. III France **5** 355-371 (1995)
7. E. j. Meijer, M. Matters, P. T. Herwig, D. M. de Leeuw and T. M. Klapwijk, *Appl. Phys. Lett*. 23, 76 (2000)
8. P. Stallinga, H. L. Gomes, F. Biscarini, M. Muriga and D. M. de Leeuw, J. *Appl. Phys*. 9, 96 (2004)
9. R. J. Chesterfield, J. C. Mackeen, C. R. Newman and C. D. Frisbie, J. *Appl. Phys*. 11, 95 (2004).
10. P. Stallinga, H. L. Gomes, Organic Electronics 6, 137-141 (2005).
11. G. Horowitz and M. E. Hajlaoui Adv. Mater. 12, 14, 1046-1050 (2000).
12. M. C. J. M. Vissenberg and M. Matters, Phys. Rev. B **57**, 12964 (1998).
13. R. Metselaar and G. Oversluizen, J. Solid State Chemistry, 55, 320-326 (1984).
14. W. Meyer and H. Neldel, *Z. Tech*. 18, 588 (1937)
15. J. C. Wang and Y. F. Chen, *Appl. Phys. Lett*. **73**, 948 (1998).